Comparison of Operating Mechanisms for the Poly(*N*-vinylcarbazole) Based Non-Volatile Memory Devices

*Jin-Sik Choi, Dong Hack Suh**

Summary: The organic non-volatile memory devices (NVMs) based on poly(*N*-vinylcarbazole) (PVK) with the different structures and compositions were fabricated and evaluated. The resistance states in the devices were controlled by the external electric field and exhibited the distinctive properties; the device with a single PVK layer was a write-once read-many-times memory by the field induced filament as a conduction path and its memory properties depended on the PVK thickness, the PVK/Al/PVK structured device was operated by a space charge limited current model and was sensitive to preparing condition of the internal Al layer, and the device performances with the PVK based charge transfer complex depended on the composition of the CT materials and the surface condition of the bottom electrode.

Keywords: charge transfer; filament; organic non-volatile memory devices; space charge limited current; thin Film

Introduction

In recent years, many investigators have focused on the organic electronics such as organic light emitting diodes (OLEDs), organic thin film transistors (OTFTs), and organic solar cells because of low-costs, flexibility, and integration into the large area.[1–7] The scope of organic electronics was even extended to the non-volatile memory devices (NVMs) which employed the organic and polymeric materials as active layer; an organic or polymeric single layer,[8–10] organics in a polymer matrix,[11–13] a thin metal layer between organic layers,[14–16] nanoparticles in polymer,[17,18] an organic based charge transfer complex,[19–21] and so on. The operations of these devices have been interpreted by the filament (F) model,[9–11] the space charge limited current (SCLC) model[14–16,18] and the charge transfer (CT) model.[8,12,13,17,19–21] In addition, it has been reported that the memory effect was induced by metallic defects from the vulnerable processes for the fabrication of device.[22]

Even though the various models were proposed, it is difficult to clearly classify them because the devices were fabricated by the organic materials with different functional groups and by the dissimilar processes. In this report, we investigate the major fabrication parameters and the operation properties using the different organic NVMs based on poly(N-vinylcarbazole) (PVK).

Experimental Part

The separated single cell without the cross-talking problem was prepared for these experiments as shown the Figure 1.

The types of the active layers were a single PVK layer (SPL) for the F model, a thin aluminum (Al) layer between PVK layers (MPL) for the SCLC model, and a PVK based CT complex layer (CTL) for the CT model. Here, the applied substances were PVK, deposited thin Al and 2,4,7-trinitro-9-fluorenone (TNF).

The devices were usually prepared and examined by the following sequences and

Department of Chemical Engineering, Hanyang University, Seoul 133–791, Korea
Fax: +82-2-2220-4523;
E-mail: dhsuh@hanyang.ac.kr

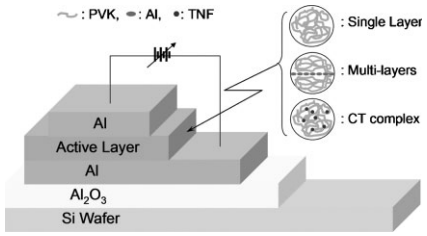

Figure 1.
Schematic diagram of organic non-volatile memory devices consisting of different active layers based on PVK; a single PVK layer (SPL), a thin metal layer between PVK layers (MPL), and a TNF:PVK CT complex layer (CTL).

tools. 50 nm-Al as the bottom electrode was formed after depositing 50 nm Al_2O_3 film as an insulator layer on a silicon wafer. The 50 nm-polymer layer was coated by the spin casting method on the bottom electrode. The polymer coated samples were dried in a vacuum oven at 50 ° for 30 min to evaporate the solvent as 1,2-dichloroethane. In case of the CTL device, the TNF:PVK mixture was coated after the samples with the bottom electrode carried out the heat treatment at 400 ° for 2 hours. The 50 nm-PVK layers in the MPL device were coated before and after deposition of the internal thin Al layer. The top electrode was deposited 50 nm-Al on the active layer. The active area of each device was typically defined 1 mm^2 by the depositions of the electrodes using the shadow masks. The fabricated devices were characterized by semiconductor analyzer HP 4155A for current-voltage (I-V) measurement, 1255A frequency response analyzer for impedance-frequency (I-F) properties and HP 4263B LCR Meter for capacitance-voltage (C-V) measurement at 100 KHz. All electric evaluations were carried out at room temperature and in a black box without light.

Results and Discussion

In I-V measurement to investigate the basic electric properties, three models showed the analogous switching behaviors as shown in Figure 2; the devices were changed from a high resistance state (OFF state) to a low resistance state (ON state) by the abruptly increased currents during the forward bias scan and also returned to OFF state during the reverse bias scan.

But the SPL device was a write-once read-many-times (WORM) memory device which was unexpected.[10] The pristine device was switched from OFF state to ON state at 1.8 V during the forward bias scan. In particular, most devices with less than 50 nm of PVK single layer showed the WORM properties. The thickness of the active layer was a critical condition to realize the WORM properties in the SPL device. This switching phenomenon to a low resistance state could be originated from the diffused metals during the electrode deposition.[9,22] But it was insensitive to the deposition rate of top electrode which was changed from 0.1 Å/sec to 3 Å/sec. In contrast, the MPL and the CTL devices revealed the reversible switching properties. In the MPL device, the switching properties were very sensitive on the preparing conditions of the internal Al layer. The reproducible device was only observed at an internal Al layer with 5 nm thickness which was deposited by 0.8 Å/sec in our case. Also, the MPL devices sometimes showed the intermediate states between the ON and the OFF states during electric operations. These phenomena would be caused by a irregularity of the thin internal metal layer which consisted of metal particles with the different granular size.[15,18] Unlike the MPL devices with these unstability, the CTL devices showed a relatively stable switching behavior and their major parameters to realize a device were the composition of CT substances and the surface condition of the bottom electrode; 0.6:1 of TNF:PVK in the mole ratio was effective to maximize the ON/OFF ratio since it was the composition around the highest density of CT complexes in the mixture, and the oxidized bottom electrode was also useful to stabilize the ON/OFF current by polarity compensation of the active layer in each state[21].

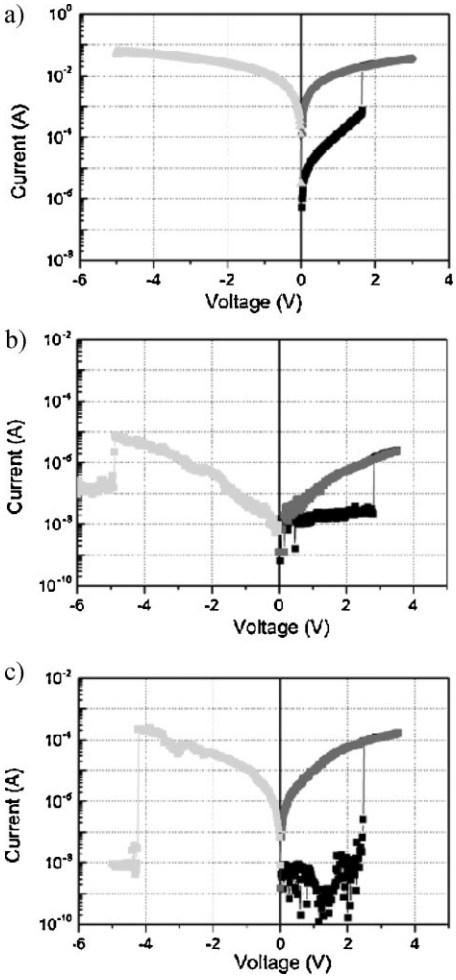

Figure 2.
I-V characteristics of three different devices based on PVK; (a) the SPL device, (b) the MPL device, (c) the CTL device.

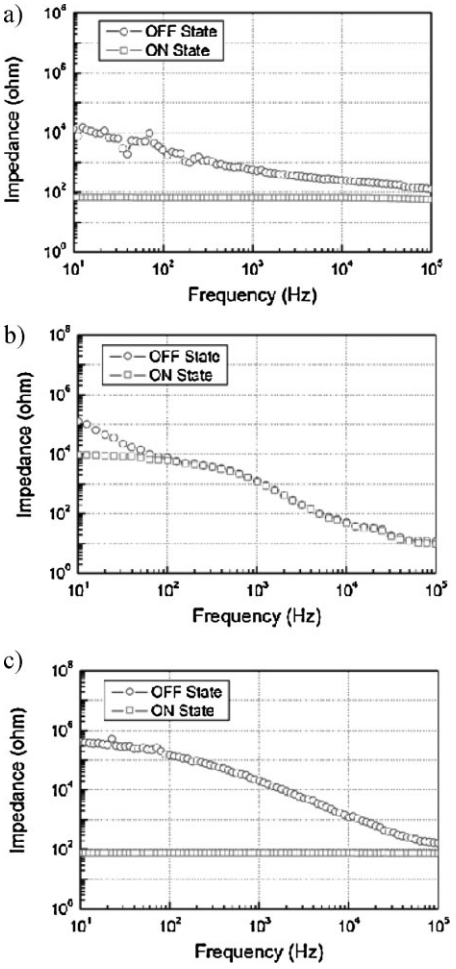

Figure 3.
Typical impedances of the devices with frequency from 10 to 10^5 Hz; (a) the SPL device, (b) the MPL device, (c) the CTL device.

According to the above I-V results, the SPL device had a WORM property and the others worked the reversible NVMs. To confirm their conduction mechanisms, we investigated the alternating-current (AC) properties such as the frequency dependencies and the capacitance variations in the same devices.

As shown in the Figure 3, the impedances of the SPL and the MPL devices in the OFF state seemed to be proportional to $1/(\omega C)$ such as a dielectric characteristic, where ω is the angular frequency and C is the capacitance. But the impedances of the CTL device in the OFF state appeared somewhat independent in the low frequency. Therefore, the CTL device might only possess charge carriers in the active layer even in the OFF state. In case of the ON state, both SPL and CTL devices displayed the frequency independency of the impedances, which might be associated with the existence of the charge carriers. But the MPL device showed a relatively strong frequency dependency except for a low frequency region. The dependency

could be interpreted by the fact that the conductance of the MPL device was controlled by the field induced space charges[16] and performed by '' hopping'' or ''tunneling''[18] in the internal thin metal layer.

Even if the SPL and the CTL devices possess the similar frequency dependencies in the ON state, their impedances were different constitutions as shown in the Figure 4. The SPL device was closed to a resistance-capacitance (RC) parallel circuit and the CTL device was related to a RC serise cicuit. The capacitances would be caused by the pristine organic materials such as PVK and TNF:PVK CT complexes, and the resistances would be related to the generated conduction paths by the switching.

Since the impedance differences between the ON/OFF states were caused by the changes of the dielectric properties in their active layers, we observed the capacitance changes during the initial bias scans through C-V measurement. In the SPL device, the capacitance reached almost 0F at the reverse bias scan after switching around 1.8 V by the forward bias scan. The 0F would result from a filament formation as a conduction path. In the CTL device, the abrupt capacitance change was also detected around the turn-on voltage. But the capacitance was suddenly returned to the pristine level nearby the turn-off voltage unlike the SPL device. But the C-V results for the MPL device were excluded because of the complicated spectrums which would be caused by the various charging states in the internal metal layer.

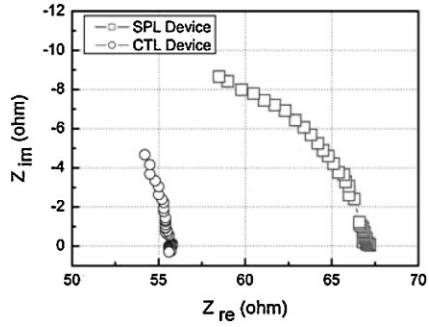

Figure 4.
Nyquist plots of the SPL and CTL devices which showed a similar impedance-frequency behavior at the ON states.

Conclusion

We prepared and evaluated three organic NVMs based on PVK with different operation models. Each device possesses the unique processing parameters and the distinct operating mechanisms. In the SPL device, the switching behavior depended on the PVK thickness and the current at ON state would arise from the field induced filament as a conduction path. In case of the MPL device as known the SCLC model,

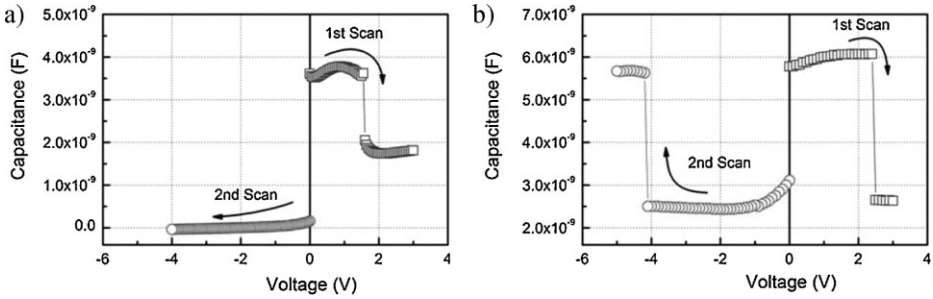

Figure 5.
The C-V characteristics of (a) the SPL device and (b) the CTL device. Arrows indicate the sweep sequences of the applied voltage. The capacitance of the SPL device reaches almost 0F at the reverse bias scan but that of the CTL device returns to a pristine value by the reverse bias scan.

the critical factor to realize the NVMs was the forming condition of the internal Al layer. The performances of the CTL device as the CT model were optimized by the control of the CT materials composition and the surface modification of the bottom electrode.

Acknowledgements: The authors are grateful to "National Program for 0.1 Terabit NVM Device" (grant No. 10022977-2004-11) supported by the Ministry of Commerce, Industry and Energy, Republic of Korea.

[1] M. A. Baldo, M. E. Thompson, S. R. Forrest, *Nature* **2000**, *403*, 750.
[2] E. Holder, B. M. W. Langeveld, U. S. Schubert, *Adv. Mater.* **2005**, *17*, 1109.
[3] C. D. Dimitrakopoulos, P. R. L. Malenfant, *Adv. Mater.* **2002**, *14*, 99.
[4] L. L. Chua, J. Zaumsell, J. F. Chang, E. C. W. Ou, P. K. H. Ho, H. Sirringhaus, R. H. Friend, *Nature* **2005**, *434*, 194.
[5] L. S. Mende, A. Fechtenkötter, K. Müllen, E. Moons, R. H. Friend, J. D. MacKenzie, *Science* **2001**, *293*, 1119.
[6] J. Roncali, *Chem. Soc. Rev.* **2005**, *34*, 483.
[7] S. R. Forrest, *Nature* **2004**, *428*, 911.
[8] Q. Ling, Y. Song, S. J. Ding, C. Zhu, D. S. H. Chan, D. L. Kwong, E. T. Kang, K. G. Neoh, *Adv. Mater.* **2005**, *17*, 455.
[9] D. Tondelier, K. Lmimouni, D. Vuillaume, C. Fery, G. Haas, *Appl. Phys. Lett.* **2004**, *85*, 5763.
[10] Y. S. Lai, C. H. Tu, D. L. Kwong, J. S. Chen, *Appl. Phys. Lett.* **2005**, *87*, 122101.
[11] L. Ma, Q. Xu, Y. Yang, *Appl. Phys. Lett.* **2004**, *84*, 4908.
[12] J. Ouyang, C. W. Chu, C. R. Szmanda, L. Ma, Y. Yang, *Nat. Mater.* **2004**, *3*, 918.
[13] C. W. Chu, J. Ouyang, J. H. Tseng, Y. Yang, *Adv. Mater.* **2005**, *17*, 1440.
[14] L. P. Ma, J. Liu, Y. Yang, *Appl. Phys. Lett.* **2002**, *80*, 2997.
[15] L. Ma, S. Pyo, J. Quyang, Q. Xu, Y. Yang, *Appl. Phys. Lett.* **2003**, *82*, 1419.
[16] L. D. Bozano, B. W. Kean, V. R. Deline, J. R. Salem, J. C. Scott, *Appl. Phys. Lett.* **2004**, *84*, 607.
[17] R. J. Tseng, J. Huang, J. Ouyang, R. B. Kaner, Y. Yang, *Nano Lett.* **2005**, *5*, 1077.
[18] L. D. Bozano, B. W. Kean, M. Beinhoff, K. R. Cater, P. M. Rice, J. C. Scott, *Adv. Funct. Mater.* **2005**, *15*, 1933.
[19] W. Xu, G. R. Chen, R. J. Li, Z. Y. Hua, *Appl. Phys. Lett.* **1995**, *67*, 2241.
[20] R. Kumai, Y. Okimoto, Y. Tokura, *Science* **1999**, *284*, 1645.
[21] T. Oyamada, H. Tanaka, K. Matsushige, H. Sasabe, C. Adachi, *Appl. Phys. Lett.* **2003**, *83*, 1252.
[22] W. Tang, H. Shi, G. Xu, B. S. Ong, Z. D. Popovic, J. Deng, J. Zhao, G. Rao, *Adv. Mater.* **2005**, *17*, 2307.

